AN IMPROVED PERTURB AND OBSERVE MAXIMUM POWER POINT TRACKING TECHNIQUE USING FUZZY LOGIC CONTROLLER

E. A. Kisame[1], M. J. Gatari[2], D. M. Mulati[3] and M. Lavi[4]
[1]Institute of Nuclear Science and Technology, University of Nairobi
[2]Institute of Nuclear Science and Technology, University of Nairobi
[3]Institute of Energy and Environmental Technology, Jomo Kenyatta University of Agriculture and Technology
[4]Department of Technical and Applied Physics, Technical University of Kenya

Abstract
In this work, an improved microcontroller-based maximum power point tracking algorithm for PV solar charge controller is proposed and implemented. The proposed algorithm uses fuzzy logic controller to adaptively modify the step-size of a conventional P&O algorithm, thereby improving its transient and steady-state responses. The proposed algorithm is implemented in a prototype solar charge controller consisting of a solar panel, a buck converter and a microcontroller. The results of the tests performed on the proposed algorithm are compared to those of a conventional P&O algorithm and a PV system with no MPPT, to validate the algorithm. The comparison with the conventional P&O algorithm shows 93% and 72% improvements in transient and steady-state responses, respectively, while that with no MPPT shows 71% improvement in efficiency with which the proposed algorithm extract energy from a solar panel.

Key words: maximum power point tracking (MPPT), fuzzy logic control (FLC), photovoltaic (PV), buck DC-DC converter

1.0 Introduction

The most viable of the solar energy technologies is photovoltaic solar panel which converts solar energy directly to electricity. Solar panels are used in many applications such as battery charging, lighting, water pumping, and satellite power systems (Dolara et al., 2009). The panels have the advantage of being maintenance and pollution free but their main drawbacks are high fabrication cost and low energy conversion efficiency (Mohammad et al., 2002). Since solar panels still have relatively low energy conversion efficiency, their overall system size and cost can be reduced by using Maximum Power Point Tracking (MPPT) algorithms which are designed to extract the maximum possible power from the solar panels (Nazih et al., 2009). Many MPPT algorithms have been proposed such as Incremental Conductance, Constant Voltage, Neural Network (Divyansh, 2014) and Fuzzy Logic Controller (Basil and Mohammed, 2012) These algorithms have some disadvantages such as dependency on solar cell configuration and complexity in implementation.

The Perturb and Observe (P&O) is the most known and commercially used MPPT technique due to its simplicity and ease of implementation (Khandker et al., 2013). Moreover, it is independent of solar cells configurations and technology, and is therefore applicable to all types of solar panels. However, it mainly suffers from steady state power oscillations as it continues perturbing the reference variable even when the steady state is reached. In addition, when the P&O technique is applied, the size of the deviation while oscillating about the MPP is determined by the perturbation step-size; having a large step-size leads to a better transient response (i.e. faster tracking), but results in large power oscillations in the steady-state. On the other hand, the choice of a small step-size leads to a slower transient response but less power oscillations at the steady state. Consequently, the selection criterion of the step-size is based on the best trade-off between the transient response speed and the steady-state oscillation.

In an effort to resolve the ambiguity of choosing the proper step-size value, this study proposes a fuzzy-based adaptive step-size algorithm. This algorithm adjusts the step-size value of the P&O algorithm according to the position of the solar panel's operating point. Thus, a large step-size value is set when the operating point is away from the MPP and vice-verse. Consequently, this assures a fast transient response, in addition to small power oscillations at the steady state (Bader et al., 2011).

The rest of this paper is organized as follows. Section 2 discusses the theory of PV solar panel, buck converter and the proposed fuzzy-based P&O algorithm. Section 3 describes the methodology used to implement the proposed algorithm. Experimental results are presented and discussed in section 4 while the conclusions are drawn in section 5.

1.0 Theory

1.1.1 Photovoltaic Solar Panel

The current versus voltage (I/V) curves of a typical solar panel under different insolation levels are shown in Fig.1.

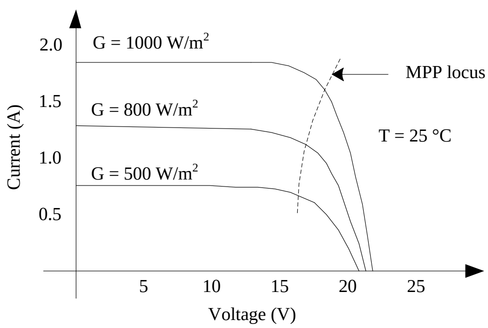

Fig. 1: I/V curves of a solar panel for various insolation levels at a temperature of 25°C

For a given insolation level, the solar panel can be considered as a current source for voltages ranging from zero to the knee of the I/V curve. It can be considered as a voltage source when it is operating close to the point of open circuit voltage. When the operating point is close to the knee of the curve, the solar panel will be approaching its Maximum Power Point (MPP). This can be seen on the corresponding power versus voltage (P/V) curves of the solar panel, shown in Fig. 2 (Geoff, 2001). It shows that increasing the insolation level increases the output power and vice versa.

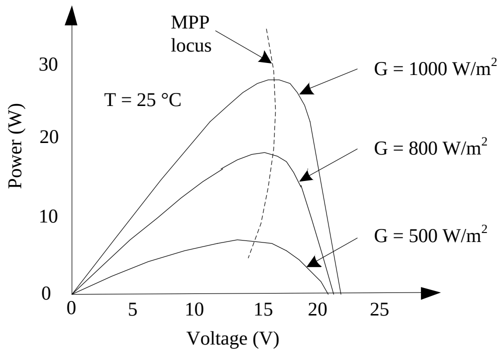

Fig. 2: P/V curves of a solar panel for various insolation levels at a temperature of 25°C

1.1.2 Buck Converter

A buck converter is a direct-current to direct-current (DC-to-DC) converter which transforms an input voltage into a lower regulated voltage in the same polarity and is not isolated between input and output (Swapnil and Subroto, 2013). It basically consists of an output capacitor C, power switch Q, diode D, inductor L and a drive circuit, as shown in Fig. 3. The inductor and capacitor make up the output filter. The resistor R_L represents the load seen by the buck converter output. The drive circuit generates a Pulse Width Modulated (PWM) signal that drives the power switch Q ON or OFF (Vladimir, 2014). V_{in} is the input voltage and V_{out} is the buck converter output voltage.

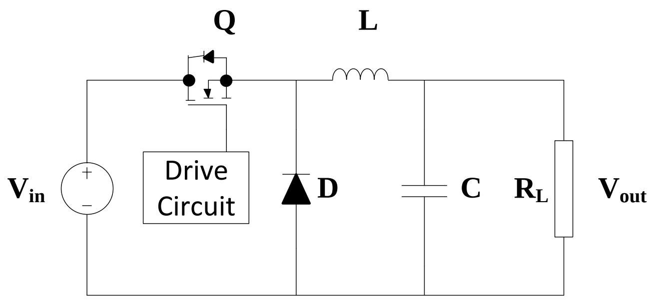

Fig 3: A circuit diagram of a buck converter

The buck converter alternates between connecting the inductor to the input voltage to store energy in the inductor when the PWM signal is high and discharging the inductor into the load when the PWM signal is low. When the PWM signal is high, the power switch becomes ON and the diode OFF. The current flows from the input power source, through the switch and the inductor to the load. The output capacitor smoothens out ripples present in the output voltage. During this time, energy is stored into the inductor in the form of a magnetic field. When the PWM signal is low, the power switch becomes OFF and the diode ON. The input voltage is isolated from the rest of the circuit. In order to maintain current to the load, the magnetic energy in the inductor is transformed into a current. The current flows from the ground through diode and inductor to the load.

1.1.3 Fuzzy-based P&O Algorithm

Maximum Power Point Tracking (MPPT) is a method used to harness the maximum power from a solar panel. The method is based on the P/V characteristic curves of a solar panel. The point on the curve where the power is maximized is called the Maximum Power Point (MPP). By inserting a DC-to-DC converter between the solar panel and a load, the voltage of the solar panel can be controlled to operate at the MPP and thus deliver maximum power to the load (Ratna and Rifa'i, 2012).

The proposed fuzzy-based P&O algorithm builds upon the simplicity of the conventional P&O algorithm but eliminates the steady-state power oscillations inherent in this algorithm by adaptively modifying the perturbation step-size using a Fuzzy Logic Controller (Nabulsi and Dhaoudi, 2012). The fuzzy-based P&O algorithm consists of P&O algorithm and fuzzy-based adaptive step-size algorithm, as explained in the following sub-sections.

1.2 P&O Algorithm

Perturb and Observe (P&O) algorithm perturbs a reference voltage using a trial and error approach to get closer to the MPP (Tekeshwar et al., 2014). The operation of the P&O algorithm is explained by a flowchart given in Fig. 4

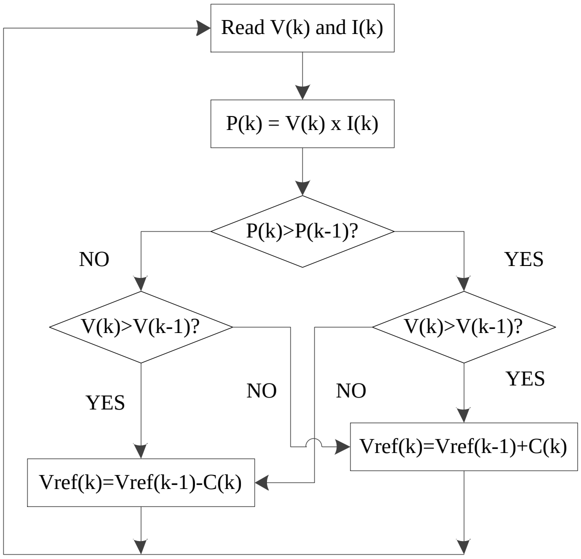

Figure 4: Flowchart of the P&O algorithm

.

From the flowchart, it is seen that the P&O algorithm periodically changes the reference voltage Vref(k) by a fixed step-size C(k) along the direction of increasing power. Firstly, the panel's output voltage V(k) and output current I(k) are sensed to calculate the output power P(k) This power is then compared to the previously calculated power P(k-1) to determine the direction of increasing power; if P(k) is greater than P(k-1) the perturbation direction is maintained, otherwise, the perturbation direction is reversed.

1.3 Fuzzy-Based Adaptive Step-Size Algorithm

The flowchart of the fuzzy-based adaptive step-size algorithm is presented in Fig.5. It comprises of four principal processes; calculation of FLC inputs, fuzzification, inference mechanism and defuzzification (Ahmad, 2004).

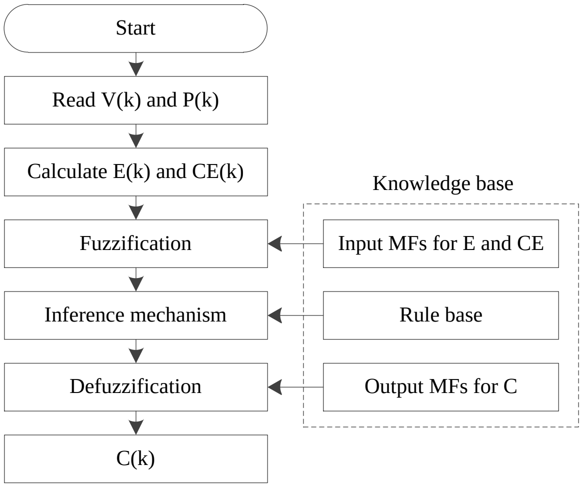

Fig. 5: Flowchart of the fuzzy-based adaptive step-size algorithm.

Calculation of FLC inputs

The algorithm calculates the slope E (k) and the change in the slope CE (k) of a P/V curve of a solar panel at each sample time k. The inputs E (k) and CE (k) are defined by Eq. (1) and (2), respectively.

$$E(k) = \frac{P(k) - P(k-1)}{V(k) - V(k-1)} \tag{1}$$

$$CE(k) = E(k) - E(k-1) \tag{2}$$

1.4 Fuzzification

Fuzzification transforms the numerical values of E (k) and CE (k) into a set of fuzzy linguistic terms based on the degree of membership of E (k) and CE (k) to each of the terms in the fuzzy set. Fig. 6 illustrates the fuzzy set of the slope E which contains 2 trapezoidal Membership Functions (MFs) and one triangular Membership Function.

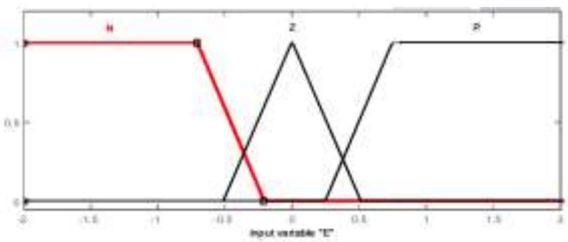

Fig. 6: Membership functions of the input variable E

Fig. 7 illustrates the fuzzy set of the change in the slope CE which contains 2 trapezoidal Membership Functions (MFs) and one triangular Membership Function.

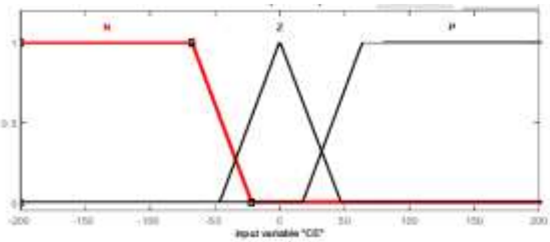

Fig. 7 Membership functions of the input variable CE

Fig.8 illustrates the fuzzy set of the output variable C which contains two triangular Membership Functions (MFs) and one trapezoidal Membership Function.

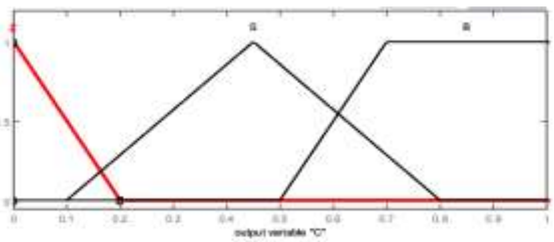

Fig. 8: Membership functions of the output variable C

1.5 Inference Mechanism

The fuzzy inference mechanism is used to evaluate and combine the IF-THEN rules in Table 1 to realize mapping from the input fuzzy sets E and CE to the output fuzzy set C. The fuzzy inference process is carried out by using Mamdani method (Cornelius, 1998).

The rules in the table are designed to achieve large step size value when the operating point is away from the MPP and vice-verse. For instance, if the value of the slope E is Negative (N), this means that the operating point is away from the MPP. The change in the slope CE can have in this case three different values. If CE is Negative (N), it implies that the operating point is moving away from the MPP. Consequently, the step-size C has to be Big (B) in order to rapidly reach the MPP. Whereas if CE is Zero (Z), it implies that the operating point is moving slowly towards the MPP, and therefore the C has to be Small (S) in order to reach the MPP without oscillating around it. Finally if CE is Positive (P), it implies that the operating point is moving rapidly towards the MPP, hence C has to be Zero (Z) in order to avoid exceeding the MPP in the opposite direction leading to oscillations. The same scenarios can be applied to the other cases shown in Table 1.

Table 1: A fuzzy rule base

CE \ E	N	Z	P
N	B	S	PB
Z	PS	ZE	PS
P	PB	PS	PB

Defuzzification

The last step in the fuzzy logic controller process is the defuzzification, which takes the output fuzzy set C and transforms it back to a real continuous number or a crisp output (i.e. the step-size value). The Center of Gravity defuzzification method is used in this work.

2.0 Materials and Methods

2.1 Hardware implementation

A schematic diagram of a prototype for a solar charge controller that was used to implement the proposed fuzzy-based P&O algorithm is shown in Fig. 9. A photograph of the hardware prototype of the solar charge controller is shown in Fig.10.

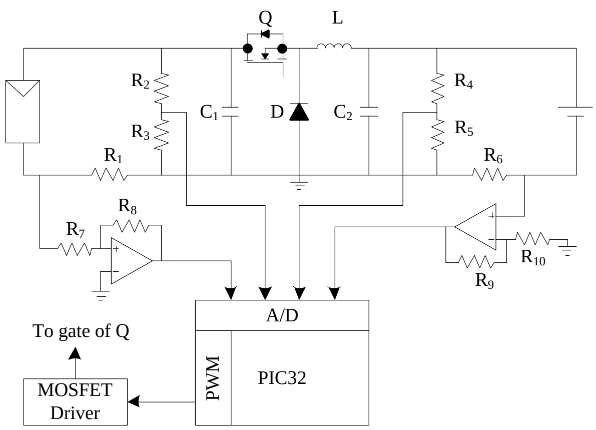

Fig.9: Schematic of solar charge controller

The circuit consists of a solar panel, a buck converter, a micro-controller, voltage and current sensors, and other peripherals for ensuring the robustness of the system. The sensors are used to periodically sample voltage and current from the solar panel. The signals from the sensors are fed into the micro-controller through the analog to digital (A/D) converter channels. The proposed algorithm running inside the micro-controller processes the voltage and current readings and calculates the duty cycle of the PWM which will operate the solar panel at its MPP. The output of the micro-controller is the PWM signal that controls the buck converter.

The buck converter is designed to operate in continuous conduction mode with the following specifications: the input and the output voltage ripples are less than 0.1V, and the peak-to-peak inductor current ripple is less than 20% of the input current. The computed component values are: L=100 μH, C_1=990 μF, C_2=1680 μF and a switching frequency of 20 KHz.

A voltage divider circuit, consisting of R_2 and R_3, is used to sense the solar panel's voltage. The values of the resistors are chosen as high as possible (i.e. multiples of 10 KΩ) in order to limit the current flowing into the divider, thus minimizing power losses. The voltage divider is designed such that its maximum output voltage does not to exceed 3.3 V when the panel is operating at its maximum voltage. The purpose of this is to protect the micro-controller which has a maximum limiting input voltage of 3.3 V.

As for the current sensor, a shunt resistor R_1 with an inverting amplifier is used to sense the solar panel's current. This amplifier produces a voltage which is directly proportional to the current going into the solar panel. Since the resistor is placed in series with the panel, its value is chosen as low as possible (0.1 Ω) to minimize the power losses in this current sensing resistor. The gain of the amplifier is set such that its output voltage do not exceed 3.3 V when the panel is operating at its maximum current.

Fig.10: A photograph of the hardware prototype

2.2 Software Development

The software development was done using the Microchip's MPLAB-X IDE v3.05, windows based integrated development environment, which allows the creation of source code using the built in editor. The MPLAB-X environment has the ability to assemble, compile and link the source code using various language tools. This environment also allows the user to debug the executable logic while watching program flows with a simulator. The proposed fuzzy-based P&O algorithm was written in C language, compiled with MPLAB-X and programmed into the PIC32MX170F256B microcontroller using PICkit3.

2.3 Solar Panel Specifications

The solar panel used in this research is a 30-Watt CS6F-30P panel, which consists of 36 PV cells. The electrical specifications of this module at standard test conditions are as follows; open-circuit voltage V_{oc} = 21.7 V, short-circuit current I_{sc} = 1.92 A, maximum power voltage V_{mp} = 17.3 A, maximum power current I_{mp} = 1.73 A.

2.4 Artificial Light Source

In this study, an artificial light is used to simulate the natural sunlight. This is in order to create a fixed test conditions for comparison purposes. The artificial light consists of twelve 100-watt incandescent bulbs. The light source produced 250 W/m^2 of light intensity at a distance of 0.5m from the source.

3.0 Results and Discussion

In order to verify the functionality of the proposed fuzzy-based P&O algorithm, several tests were conducted under similar conditions of light and temperature. As mentioned in the previous section, an artificial light was used to simulate the natural sun. It produced around 8.16 W of electricity from CS6F-30P Solar Panel. A 5Ω resistor was used as a load. The results of the experiments were recorded by use of two multimeters with data-logging capability, at an interval of a second. In the both tests, the output voltage $V_{pv}(k)$ and the output current $I_{pv}(k)$ of the solar panel were recorded periodically for 250 seconds and the output power $P_{pv}(k)$ was calculated using the formula: $P_{pv}(k) = V_{pv}(k) \times I_{pv}(k)$.

3.1 Results of Fuzzy based P&O Algorithm

In the first test, the proposed fuzzy-based P&O algorithm was implemented in the hardware prototype of the solar charge controller. From the test, the panel's output voltage, current and power are shown on Table 2. Fig.11 is plotted using the values in Table 2.

The output voltage starts dropping from around 21.5 V till it reaches the maximum power voltage V_{mp} (approximately 16.33 V). Similarly, the output current starts rising from 0 A till it reaches the maximum power current I_{mp} (approximately 0.50 A).

As can be seen in Fig.11, the maximum power P_m (approximately 8.12 W) is achieved after 10 seconds. This maximum power corresponds to the maximum power voltage and the maximum power current (i.e. $P_m = I_{mp} \times V_{mp}$).

Table 2: The experimental outputs of the solar panel when using fuzzy-based P&O algorithm

Time(s)	Voltage(V)	Current(A)	Power(W)
0	21.51	0.00	0.00
10	16.22	0.50	7.96
20	16.24	0.50	8.03
30	16.63	0.48	8.01
40	16.32	0.49	8.05
50	16.49	0.49	8.00
60	16.29	0.49	7.96
70	16.22	0.50	8.04
80	16.10	0.51	8.18
90	16.51	0.49	8.07
100	16.39	0.49	8.10
110	16.49	0.50	8.21
120	16.29	0.51	8.24
130	16.22	0.50	8.04
140	16.10	0.51	8.17
150	16.51	0.49	8.15
160	16.39	0.50	8.13
170	16.49	0.49	8.15
180	16.32	0.50	8.20
190	16.46	0.48	8.31
200	16.39	0.51	8.22
210	16.22	0.50	8.04
220	16.46	0.48	8.31
230	16.24	0.50	8.09
240	16.22	0.50	8.04
250	16.51	0.49	8.07

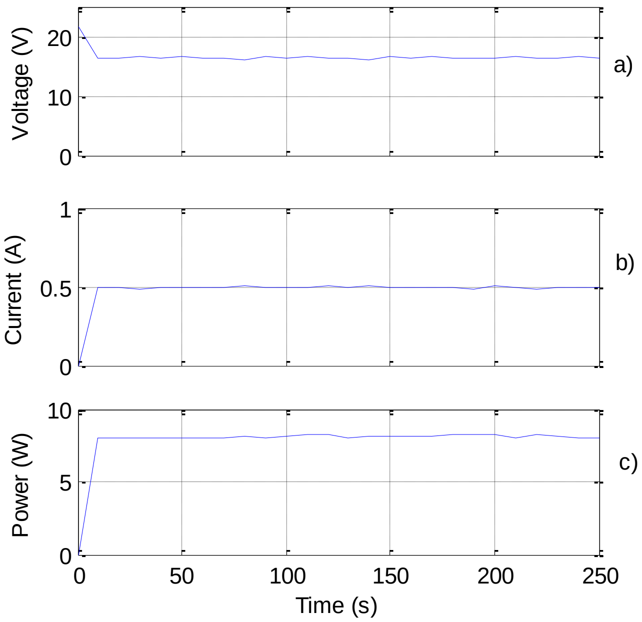

Fig.11: The experimental outputs of the solar panel when using fuzzy-based P&O algorithm

3.1 Comparison with the Conventional P&O Algorithm

In order to evaluate the performance of the proposed fuzzy-based P&O algorithm, its response was compared to that of the conventional P&O algorithm tested under similar conditions. The conventional P&O algorithm was tested at step-sizes of 0.07V and 0.6V, respectively. The comparison of the algorithms responses are shown in Table 3. Fig.12 is plotted using the values in Table 3.

Time (s)	fuzzy-based P&O algorithm (W)	P&O algorithm with a step-size of 0.07V (W)	P&O algorithm with a step-size of 0.6V (W)
0	0.00	0.00	0.00
10	7.96	6.66	8.12
20	8.03	7.01	7.90
30	8.01	6.81	8.21
40	8.05	6.80	7.93
50	8.00	7.13	8.29
60	7.96	7.35	7.65
70	8.04	7.42	7.58
80	8.18	7.59	8.20
90	8.07	7.75	8.10
100	8.10	7.84	8.10
110	8.21	7.83	7.59
120	8.24	7.82	8.24
130	8.04	7.84	8.32
140	8.17	8.13	7.48
150	8.15	8.15	8.35
160	8.13	7.98	8.25
170	8.15	8.22	7.43
180	8.20	8.15	8.17
190	8.31	8.25	8.37
200	8.22	8.22	8.14
210	8.04	7.98	8.19
220	8.31	8.17	7.43
230	8.09	8.15	8.03
240	8.04	8.09	8.34
250	8.07	8.06	8.23

Table 3: Comparison with the conventional P&O Algorithm

Referring to the results, it is observed that both the proposed fuzzy-based P&O algorithm and the large step-size P&O algorithm attain the maximum power at 10 seconds, as the small step-size P&O algorithm attains the maximum power at 150 seconds. From the results, it is deduced that the large step-size P&O and the proposed fuzzy-based P&O algorithms have comparatively fast transient response while the small step-size P&O algorithm suffers from slow transient response. Compared to the small step-size P&O algorithm, the proposed algorithm improves transient response by 93%.

At the steady-state (i.e. between 150 seconds and 250 seconds), the calculated standard deviations for both the small step-size P&O and fuzzy-based P&O algorithms is 0.09V. The small values in standard deviation indicate that the individual operating points of the two algorithms are close to the MPP, leading to minimal power fluctuations. On the contrary, the calculated standard deviation for the large step-size P&O algorithm is 0.32V, which is relatively large and indicates that there is a wide variance between the individual operating points and the MPP. This is evidently shown by the presence of large power fluctuations at the steady state, which leads to a significant energy loss in the long run. Compared to the large step-size P&O algorithm, the proposed algorithm improves the steady-state response by 72%.

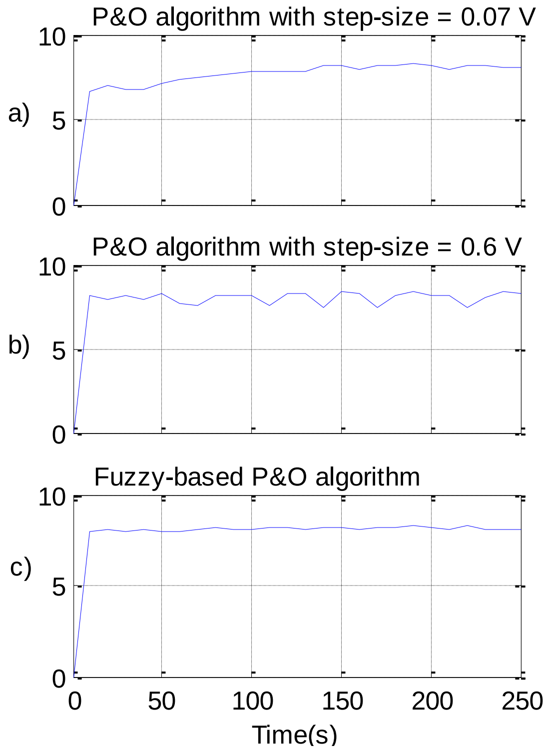

Figure 12: Comparison between Fuzzy based P&O algorithm and conventional P&O algorithm

From the analyses of the results, it is noted that the proposed fuzzy-based P&O algorithm matches the performance of the large step-size P&O algorithm in transient response and that of small step size P&O algorithm in steady state response.

3.3 Comparison with no MPPT

The test results of the output power with the proposed fuzzy-based P&O algorithm and with no MPPT are compared in Table 4. Fig.13 is plotted using the values in Table 4.

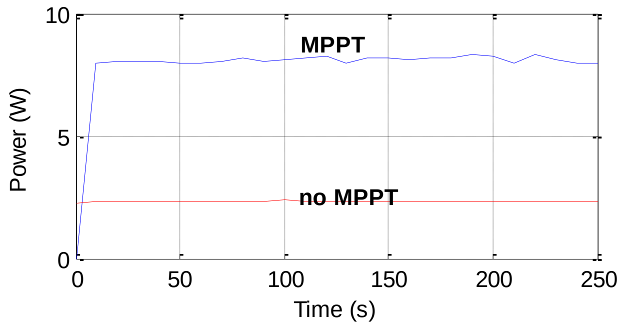

Figure 13: Comparison of output power with and with no MPPT

Table 4: The experimental outputs of the solar panel when using fuzzy-based P&O algorithm

Time (s)	fuzzy-based P&O algorithm (W)	No MPPT (W)
0	0.00	2.28
10	7.96	2.35
20	8.03	2.33
30	8.01	2.33
40	8.05	2.35
50	8.00	2.35
60	7.96	2.35
70	8.04	2.33
80	8.18	2.35
90	8.07	2.33
100	8.10	2.36
110	8.21	2.35
120	8.24	2.33
130	8.04	2.33
140	8.17	2.33
150	8.15	2.35
160	8.13	2.33
170	8.15	2.35
180	8.20	2.33
190	8.31	2.35
200	8.22	2.33
210	8.04	2.34
220	8.31	2.35
230	8.09	2.33
240	8.04	2.33
250	8.07	2.33

As can be seen, the proposed MPPT algorithm extracts more power from the solar panel (about 8.16 W), compared to when no MPPT algorithm is used, which is around 2.34 W. This corresponds to an efficiency improvement of 71%.

4.0 Conclusions

This work has proposed and implemented an improved microcontroller-based maximum power point tracking algorithm for PV solar charge controller. The proposed algorithm uses fuzzy logic controller to adaptively modify the step-size of a conventional P&O algorithm, thereby improving its transient and steady-state responses. The proposed algorithm has been implemented in a prototype solar charge controller consisting of a solar panel, a buck converter and a microcontroller. The experimental results of tests conducted on the proposed algorithm have been compared to those of a conventional P&O algorithm and a PV system with no MPPT to validate the algorithm. Analyses of the results show that the proposed algorithm improves the transient and steady-state responses of the conventional P&O algorithm by 93% and 72%, respectively. In addition, the algorithm extracts 71% more power from a solar panel as compared to when no MPPT algorithm is used.

References

Ahmad M. Ibrahim (2004). Fuzzy Logic for Systems Applications. Burlington MA 01803, Elsevier Science, ISBN 0-7506-7699-X, pp.23-48.

Bader N. Alajmi, Khaled H. Ahmed, Stephen J. Finney and Barry W. Williams (2011). Fuzzy-Logic Control Approach of a Modified Hill-Climbing Method for Maximum Power Point Tracking in Micro-grid Standalone Photovoltaic Systems. IEEE Transactions on Power Electronics, 26(4): pp.1022-1030.

Basil M. Hamed and Mohammed S. El-Moghany (2012). Fuzzy Controller Design Using FPGA for Photovoltaic Maximum Power Point Tracking. International Journal of Advanced Research in Artificial Intelligence, 1(3): pp.14-23.

Cornelius T. Leondes (1998). Fuzzy Logic and Expert Systems Applications. San Diego, California 92101-4495 USA, Academic Press Limited. ISBN 0-12-443866-0: pp.58-64.

Divyansh Mathur (2014). Maximum Power Point Tracking with Artificial Neural Network. International Journal of Emerging Science and Engineering, 2(**3**): pp.38-42.

Dolara A., Faranda R., and Leva S.(2009). Energy comparison of seven MPPT techniques for PV system. J. Electromagnetism Anal. Appl. 1(3): pp.152-162.

Geoff Walker (2001). Evaluating MPPT Converter Topologies Using a Matlab PV Model. Journal of Electrical and Electronics Engineering, Australia, 21(**1**): pp.49-56.

Khandker Tawfique Ahmed, Mithun Datta and Nur Mohammad (2013). A Novel Two Switch Non-inverting Buck-Boost Converter based Maximum Power Point Tracking System. International Journal of Electrical and Computer Engineering, 3(**4**): pp.467-477.

Nabulsi A., and Dhaouadi R. (2012). A Comparison of two MPPT techniques for PV system. WSEAS Transaction on Environment and Development, 5(**12**): pp.770-779.

Ratna Ika Putri and M. Rifa'i (2012). Maximum Power Point Tracking Control for Photovoltaic System Using Neural Fuzzy. International Journal of Computer and Electrical Engineering, 4(**1**): pp.75-81.

`